Schweizerische Eidgenossenschaft
Confédération suisse
Confederazione Svizzera
Confederaziun svizra

Department of the Environment, Transport, Energy and Communication DETEC

Swiss Federal Office of Energy SFOE
Energy Research

Final report 2018

SolAir-3

Innovative solar collectors for efficient and cost-effective solar thermal power generation – 3

Date: June 2018

Town: Manno

Publisher:
Swiss Federal Office of Energy SFOE
XY Research Programme
CH-3003 Bern
www.bfe.admin.ch

Agent:
Airlight Energy Holding SA
Via Croce, 1, CH-6710 Biasca
www.airlightenergy.com

SUPSI – DTI – MEMTi
Via Cantonale, Galleria 2, CH-6928 Manno
www.supsi.ch ; www.supsi.ch/memti

ETHZ – Institute of Energy Technology
ML J 42.1, Sonneggstr. 3, CH-8092 Zurich
www.ethz.ch , www.iet.ethz.ch

Author:
Maurizio C. Barbato, SUPSI – DTI – MEMTi, maurizio.barbato@supsi.ch
Davide Montorfano, SUPSI – DTI – MEMTi, davide.montorfano@supsi.ch
Simone A. Zavattoni, SUPSI – DTI – MEMTi, simone.zavattoni@supsi.ch
Filippo Contestabile, SUPSI – DTI – MEMTi, filippo.contestabile@supsi.ch
Aldo Steinfeld, ETHZ–IET, aldo.steinfeld@ethz.ch
Andrea Pedretti, Airlight Energy Manufacturing SA, andrea.pedretti@airlightenergy.com

SFOE head of domain: Stefan Oberholzer, stefan.oberholzer@bfe.admin.ch
SFOE programme manager: Stefan Oberholzer, stefan.oberholzer@bfe.admin.ch
SFOE contract number: SI/500926-01

The author of this report bears the entire responsibility for the content and for the conclusions drawn therefrom.

Swiss Federal Office of Energy SFOE
Mühlestrasse 4, CH-3063 Ittigen; postal address: CH-3003 Bern
Phone +41 58 462 56 11 · Fax +41 58 463 25 00 · contact@bfe.admin.ch · www.bfe.admin.ch

Contents

Summary

This document represents the final report of the Sol-Air 3 project. All the major activities and achievements, covering the original project work packages and tasks, were summarized with the aim of providing a general overview to the reader which, if willing to deeper investigate on these topics, can also find the references for gathering any additional information.

The main activities cover the following subjects:

- Solar collector
  - design and engineering of an array of coiled tube solar absorbers;
  - feasibility analysis of an isobaric receiver;
  - optical properties measurement and insulation optimization;
  - pneumatic arcspline primary concentrator.
- Piping modelling and optimization
- Thermal energy storage
  - CFD-based performance evaluation of a sensible thermocline TES;
  - CFD-based performance evaluation of a combined sensible-latent thermocline TES;
  - cyclic thermal performance;
  - characterization of the thermo-fluid dynamics behaviour of the TES integrated into the Ait-Baha pilot plant;
- Ait-Baha pilot plant design, construction, commissioning and testing.

List of abbreviations

CFD	Computational fluid dynamics
CSP	Concentrating solar power
ORC	Organic Rankine cycle
TES	Thermal energy storage
HTF	Heat transfer fluid

Work undertaken and findings obtained

1.1. Major achievements of the first year of the project (2014)

The aim of this paragraph is to provide an overview on the major results obtained during the first 12 months of the project. The detailed description of the activities can be found in:

"SolAir-3: Innovative solar collectors for efficient and cost-effective solar thermal power generation – 3" (SI/500926-01), Annual report, December 2014.

1.1.1. Array of coiled tube solar absorbers

An entirely novel solar receiver for parabolic trough concentrators, using air as HTF and operating at temperatures exceeding 600 °C, was designed, fabricated, tested, and numerically simulated (see Figure 1). Model validation is accomplished by comparison to experimental results in terms of the temperature distributions on the absorber tube and the external surface of the window.

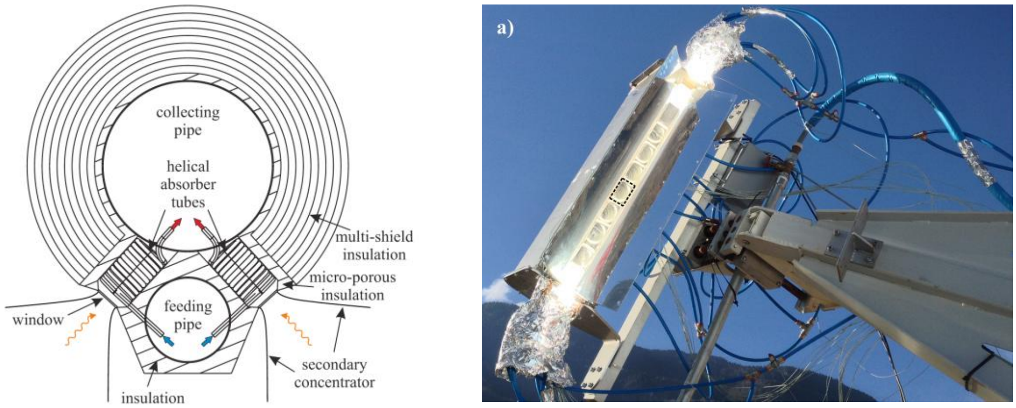

Figure 1: Receiver section with helical absorber tubes (l.h.s.) and experimental prototype (r.h.s.).

On-sun experiments were performed with a 1 m-long solar receiver prototype comprising 7 coiled absorber tubes (r.h.s. of Figure 1). With feeding rates in the range of 5-20 NL/min to each absorber tube, air outlet temperatures of 621-449 °C and receiver efficiencies of 25-64% were achieved, while the pressure drop and pumping power demand remained below 10 mbar and 1% of the expected electric power output, respectively. Major heat losses occur at the primary mirror by absorption and spillage of sunlight, at the window by solar reflection, thermal re-radiation, and natural convection, and by other loss mechanisms including conduction trough the insulation and chimney effect.

1.1.2. Isobaric receiver

The aim of the isobaric receiver is to level off the absolute pressure of the hot air in the runback pipe of a thermal solar collector. A constant value of the above-mentioned pressure is helpful in balancing the mass flow rate in each one of the numerous cavities (see Figure 2), which collect the solar radiation, without uneven temperature distribution in the whole pipe.

Figure 2: Airlight's receiver section, scheme and detail of the helically coiled heat exchangers.

To achieve an isobaric receiver a series of possible technical solutions were considered (e.g., axial fan, axial jet fan, ejector, and so on).
After a detailed analysis on the possible solutions of isobaric receiver, no further improvements were made on the design procedure. Airlight Energy found the efficiency of the axial fan previously seen not satisfactory enough. Even though its efficiency remains near 50%, no encouraging signals of greater performance were found. Consequently, the decision to stop this design research in order to instead focus on the leakage through the junctions, finding a way to minimize thermal and mass losses along the entire HTF collecting pipe.

1.1.3. Thermal energy storage system

A previously developed and validated CFD model was exploited to evaluate the thermo-fluid dynamics behavior of an industrial-scale TES system (see Figure 3) with the aim of evaluating the effect of initial consecutive charge/discharge cycles on its overall performance.

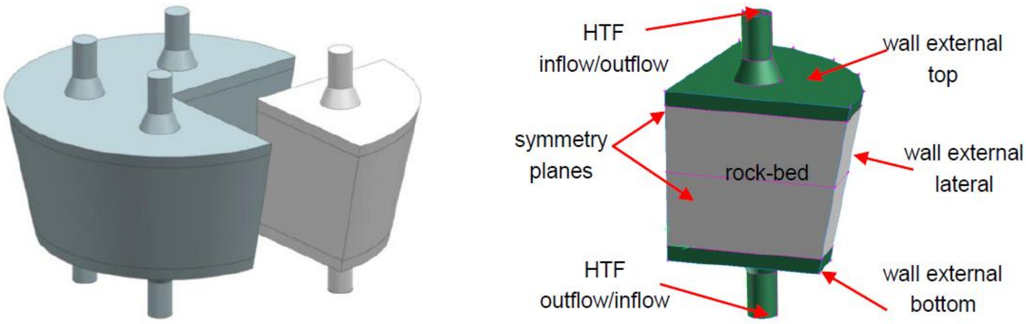

Figure 3: Computational domain of the TES under investigation (light-gray 90° slide) and main boundary conditions considered.

The 3D CFD simulation results of the TES system, analyzing 30 consecutive cycles of charging and discharging, were exploited to observe the effect of the initial cycles on the thermal stratification. The latter, qualitatively evaluated with a second-law based figure of merit, showed a strong variation lasting for 20-22 cycles. A stable thermal stratification into the packed bed was achieved towards the end of the 30 cycles analyzed. The long transient behavior is the result of the two thermocline zones, observed into the packed bed for the first 19-20 cycles, due to the fact the TES was considered in its dead state at the beginning of the test. Pre-charging the TES system before the first cycle might be a valuable solution to sensibly reduce the long time required to achieve a stable thermal stratification.

Furthermore, numerical heat transfer simulations were used to investigate a new TES concept that adds a layer of encapsulated PCM on top of a packed bed of rocks (see Figure 4). A 1D heat transfer model is formulated for the sensible and latent heat sections of the TES considering separate fluid, solid, and molten phases. The simulations indicated that a PCM volume of 1.33% of the total storage volume was sufficient to achieve stabilization of the outflow air temperature around the PCM melting point. The thermal properties of the PCM have strong influence on the behavior of the combined TES. The overall efficiency is not significantly affected by the addition of PCM.

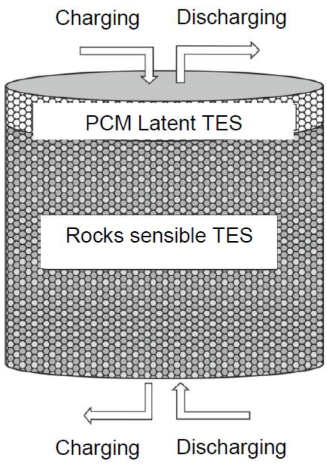

Figure 4: Schematic of the innovative concept of combined latent and sensible heat TES.

1.2. Major achievements of the first year of the project (2015)

The aim of this paragraph is to provide an overview on the major results obtained during the second year of the project. The detailed description of the activities can be found in:

“SolAir-3: Innovative solar collectors for efficient and cost-effective solar thermal power generation – 3” (SI/500926-01), Annual report, December 2015.

1.2.1. Optical properties of materials for solar concentrators

Knowledge of the optical properties of reflective materials is of paramount importance for the design of solar concentrating systems. Of interest is the reflectance weighted by the solar irradiance spectrum, which strongly affects the attainable solar concentration ratio. The optical properties of various materials for solar concentrators were measured over the solar spectrum and as a function of the incidence angle. The spectrally and directionally resolved values were then used to determine the solar-weighted specular reflectance and narrow-angle transmittance, as well as the angular scattering. These were incorporated in Monte Carlo ray-tracing simulations to elucidate their effect in the optical performance of solar concentrators. It is found that the optical efficiency and the solar concentration ratio are strongly dependent on the reflectance and transmittance of materials, while the effect of non-specularity is secondary and affects rather the solar flux distribution. For a parabolic trough concentrator of 90° rim angle and ideal geometry, the percentage decrease of optical efficiency with incident skew angle from 0° to 60° is 1% for outdoor reflectors and 10% for indoor reflectors protected by semi-transparent film covers.

1.2.2. Receiver insulation optimization

In the current layout, the insulation configuration of the collecting pipe comprises a 45 mm layer of Promaglaf® HT solid thermal insulation surrounded by twelve aluminum foils, acting as radiation shields, to further reduce the overall heat loss. An external aluminum pipe, in direct contact with the last radiation shield, encloses the whole assembly. Figure 5 illustrates a 2D cross section of the receiver showing the working principle and the current configuration of the collecting pipe insulation.

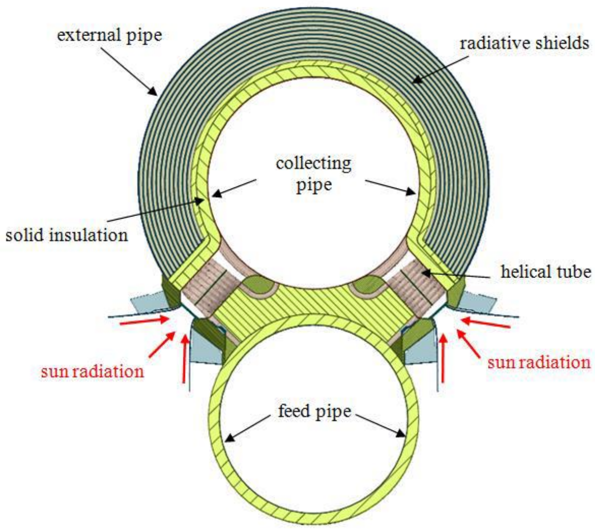

Figure 5: Receiver cross section.

The thermal insulation of the receiver collecting pipe was optimized thorough the exploitation of two different tools: (i) a purposely developed 1D analytical Matlab model and (ii) CFD-based approach. The Matlab model accounted for all the heat transfer mechanisms: conduction, convection and radiation. The results obtained for the current geometry, considered as reference case, were validated by means of accurate 2D CFD simulations, performed with Fluent code from ANSYS, showing a good agreement. However, the great reduction in terms of computational time made the analytical model really useful to compare different insulation designs during the optimization phase. The results highlighted that it is actually possible, without performance deterioration, to avoid the use of a solid insulation by rearranging the number of shields and their relative distance. However, if the shields emissivity cannot be kept low, there is a worsening of the performance which can be avoided only by increasing the number of shields at the expense of a more complex manufacturability.

1.2.3. Receiver new concepts

Due to the poor performances granted by the helical absorber tubes receiver at high skew angles, straight tubes designs were again taken into consideration. The major advantages foreseen was that they allow achieving the same heat transfer with the same pressure drop as a single absorber pipe, but with a lower temperature difference between tube walls and HTF. Some of the design proposed and analyzed are reported in Figure 6 with a visual comparison between original helical absorber tubes receiver and straight receiver shown in Figure 7.

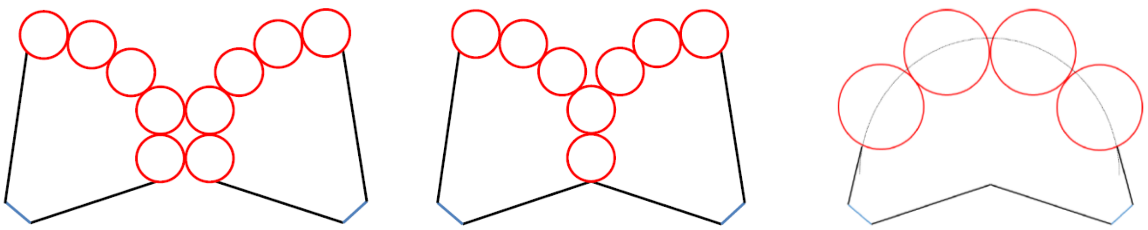

Figure 6: Schematic of straight tubes receiver designs.

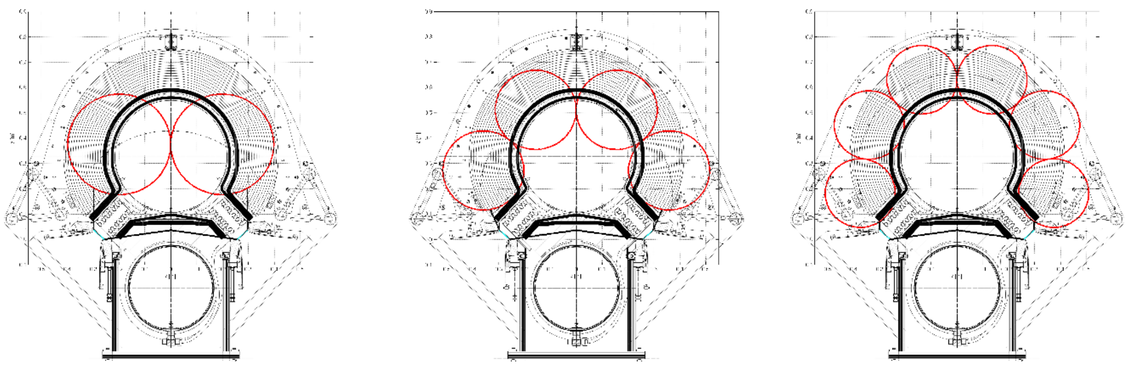

Figure 7: Cross section comparison between straight tubes and chrysalis designs.

Among the different design analysed in this chapter the best performance were shown by the one comprising two upper tubes coupled with a middle tube forming a single receiving cavity. In order to better understand the different phenomena taking place into the receiver and validate the analytical model used up to now, the best design was deeply investigated by means of CFD simulations.

1.2.4. Piping modelling

The final purpose of this task was the optimization of the piping network of a solar power plant based on Airlight parabolic trough collectors. The optimization process will lead to the best configuration in which the best trade-off among pressure drops, heat losses, exergy losses, thermal inertia is reached. These phenomena are indeed directly responsible of the operating costs during normal plant operation and the black-start time: they have to be as small as possible in order to maximize the plant productivity.
A model of the piping of a CSP plant based on the Airlight Energy technology was developed in the Simscape software environment. A representative schematic sample of the resulting scheme of a representative solar plant, based on Airlight energy technology, is reported in Figure 8. To achieve a suitable tradeoff between model completeness and performance, some Matlab calculations were left for the simulation post processing. The guidelines for the optimization process were identified in a set of simulation of topologically different layouts, based on the same geometrical definition of the components. Once the most promising layout will be identified, the geometrical optimization should be performed with an optimization tool such as Matlab or ModeFrontier since the number of parameters is relevant.

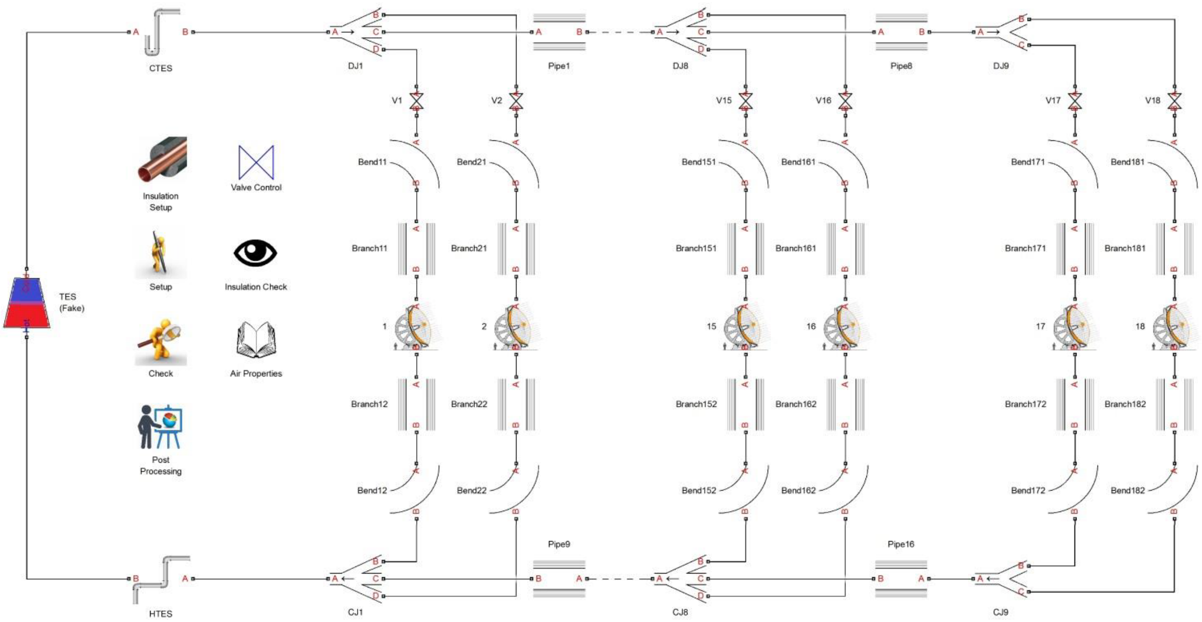

Figure 8: Overview of the piping network model.

1.2.5. Thermal energy storage system

The thermo-fluid dynamics behaviour of a single-tank TES unit (see Figure 3), with river pebble as low-cost filler material, was obtained by means of accurate time-dependent 3D CFD simulations. The system was analysed under 30 consecutive cycles of 12 h of charging followed by 12 h of discharging with constant HTF mass flow rate. To evaluate the effect of TES pre-charging on thermal stratification, three additional scenarios, characterized by 4 h, 6 h and 8 h pre-charging, were proposed and analysed with the same CFD-based approach. Besides the axial temperature distribution into the packed bed, two stratification efficiency indexes, based on the first and the second law of thermodynamics, were exploited to characterize the extent of thermal stratification. According to the CFD simulations results, the effect of pre-charging, more pronounced during the first cycles, is relevant in reducing the time required by the TES to achieve a stable thermal stratification into the packed bed. The final HTF outflow temperature during discharging is also affected by the pre-charging: at the end of the 30_{th} cycle a decrease of 7.7% and 3.7%, with respect to the nominal TES charging temperature, was observed for the TES unit with 0 h and 8 h of pre-charging respectively. However, on the basis of the HTF outlet temperature during charging, with 8 h pre-charging the TES unit resulted to be overcharged.
Concerning the transient evolution of thermal stratification, in the case of TES with 0 h pre-charging, a strong variation was observed lasting for all the 30 cycles, indicating that 30 cycles are not enough for achieving a stable thermal stratification into the packed bed. Conversely, a stable thermal stratification into the packed bed, with a MIX stratification efficiency of 0.93, was achieved after about 20 cycles and 10 cycles for the cases of 4 h and 6 h pre-charging respectively. The evolution of thermal stratification according to the entropy generation ratio showed a slightly different behavior: a stable working condition, with a stratification efficiency of about 0.67, was achieved after 22-24 cycles and 15-17 cycles in the case of 4 h and 6 h respectively.

Among the scenarios proposed, the 6 h pre-charging seems to be preferable for minimizing the time required by the TES system to achieve a stable thermal stratification with a 4% maximum decrease of the final HTF outflow temperature observable during the 30th discharging.

1.2.6. Pneumatic arcspline primary concentrator

The concept of the pneumatic arcspline concentrator that approximates the parabolic shape by a number of tangentially adjacent circular arc segments was exploited for the creation of the reflective surface to be integrated into the novel solar collector. One feature of pneumatic solar concentrators is that they allow for active mirror shape control by pressure regulation. The latest technical developments have been dedicated to the hardware and software for mirror shape regulation. A cross-section of the pneumatic arcspline trough concentrator mounted on the concrete support structure is shown in Figure 9 left. The concentrator is divided by the central concrete beam into two wings, each comprised of four mirror membranes that delimit four airtight pressure chambers. By applying appropriate pressures *p1*, *p2*, *p3*, *p4* in the chambers, the topmost membrane approximates the parabola by four tangentially adjacent circular arcs.

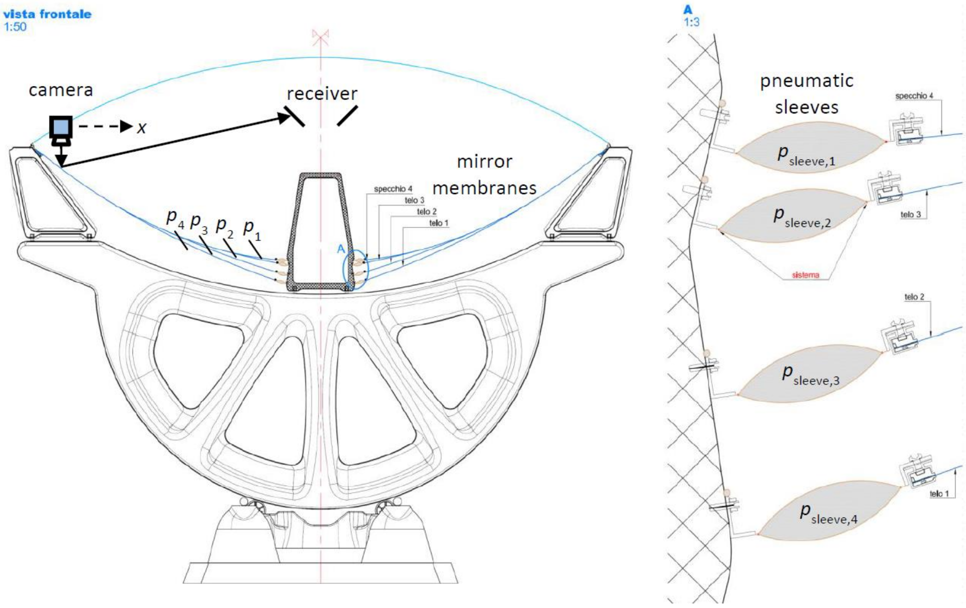

Figure 9: Cross-section of pneumatic arcspline trough concentrator comprising 2 wings composed of 4 mirror membranes mounted on the concrete support structure (left) and detail a of membrane fixture at central beam via pneumatic sleeves for arcspline shape adjustment (right).

The actuators (pneumatic sleeves) and sensors (concentrator shape measurement system) required for the active shape control of the arcspline concentrator have been developed and technically implemented at the Airlight Energy pilot plant in Ait Baha, Morocco. Arcspline shape regulation and characterization has been performed on a complete 212 m long solar collector. The average intercept factor calculated from the mirror shape measurements performed every 8.82 m on both wings is 0.77. Significant distortions of the arcspline shape occur at the weld seams of the mirror membranes and decrease the attainable intercept factor by ca. 5 – 15%. For future solar collectors this effect will be reduced or eliminated by decreasing the axial tension of the mirror membranes in the mounting process. With the primary concentrator commissioned and pressures fine-tuned, the next step is to perform on-sun tests of the concentrator in tandem with the solar air receiver and characterize the solar collector in terms of its solar-to-thermal efficiency.

1.3. Major achievements of the first year of the project (2016)

The aim of this paragraph is to provide an overview on the major results obtained during the third year of the project. The detailed description of the activities can be found in:

"SolAir-3: Innovative solar collectors for efficient and cost-effective solar thermal power generation – 3" (SI/500926-01), Annual report, December 2016.

1.3.1. Industrial scale demonstration of the solar collectors

A schematic of the solar parabolic trough concentrator is shown in Figure 10. Each of the two mirror halves is constructed from a multi-layer stack of bi-axially oriented polyester films (boPET) whose topmost film is aluminized in order to obtain a reflective surface. The mirror foils and solar receiver are mounted on a rigid concrete support structure and are protected from external impacts (e.g., wind, dust) by an inflated membrane envelope, consisting of a semi-transparent ethylene tetrafluoroethylene (ETFE) foil at the top and a polyvinyl chloride coated polyester (PVC-PES) film at the bottom.

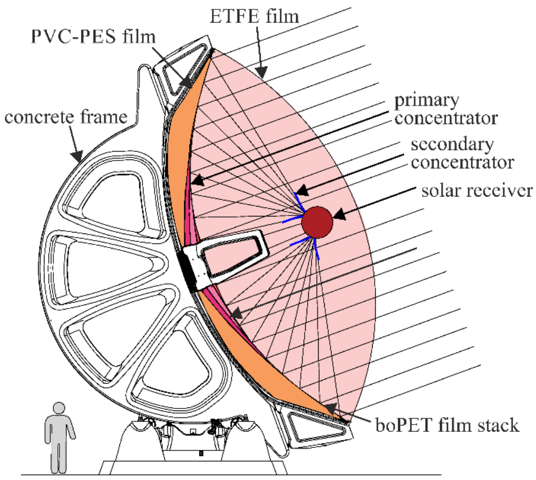

Figure 10: Schematic cross-section of solar parabolic trough concentrator comprising a pneumatic trough concentrator based on a stack of polyester films whose topmost is aluminized, a semi-transparent ETFE at the top, a PVC-coated polyester foil at the bottom, and solar receiver, all mounted on a concrete support structure.

To demonstrate the effectiveness of the proposed solar parabolic trough concentrator, a first solar plant was constructed in Ait Baha, Morocco (30.2174° N, 9.1493° W, altitude: 256 m). The layout of the plant is shown schematically in Figure 11, along with photographs of the plant and a solar collector in tracking mode (Figure 12). It is composed of three 212 m-long solar collector units, integrated to a thermal energy storage (TES) based on a thermocline packed bed of rocks that is immersed in the ground. The solar field has a total active aperture area of 5880 m^2. It provides thermal power to the TES and to an air-to-oil heat exchanger coupled to an organic Rankine cycle (ORC) for the purpose of boosting electricity production from waste heat of a cement factory.

The concrete frame of each solar collector unit is built as an assembly of 12 elementary modules, each 17.64 m-long, which constitute the basic constructive element of a pre-cast, pre-stressed fiber-reinforced high-performance concrete, manufactured on site. Each module comprises one central and two external longitudinal beams that are supported at either ends by concrete wheels based on a foundation group for decoupling the permanent load (~140 tons/module) from transient phenomena such as wind, thermal expansion, or seismic action. Each wheel is driven by a dedicated electric engine via a gearbox and precision-encoders. In addition, the torsions in all driving shafts are monitored by torsion elements. The tracking mechanism guarantees a tracking accuracy of ± 0.05°.

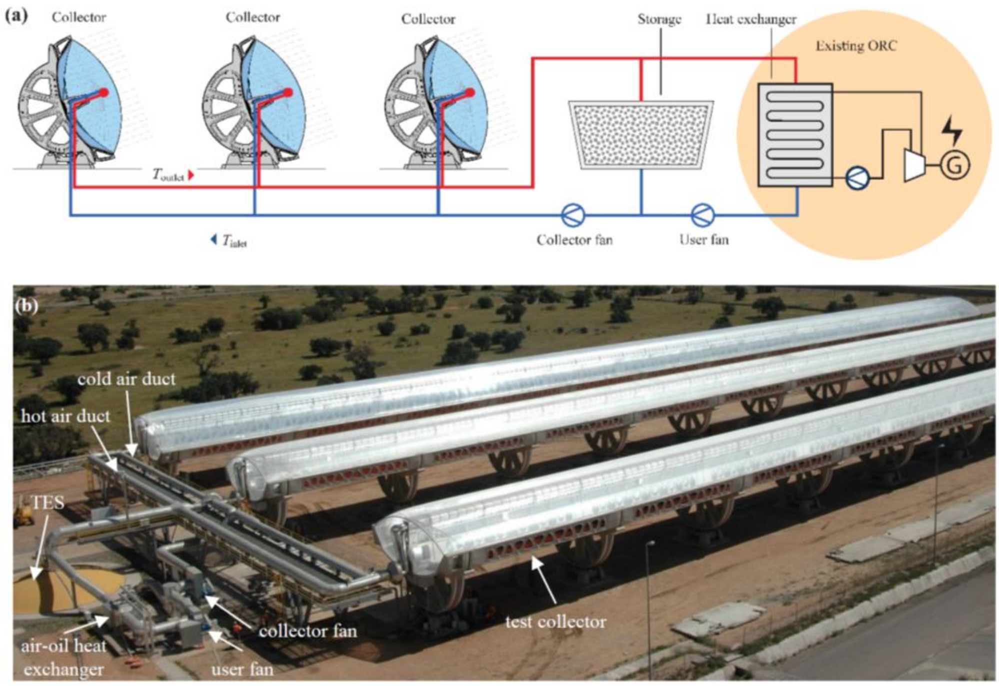

Figure 11 Pilot plant in Ait Baha, Morocco: (a) scheme; (b) photograph of the three solar trough concentrators, piping, and TES.

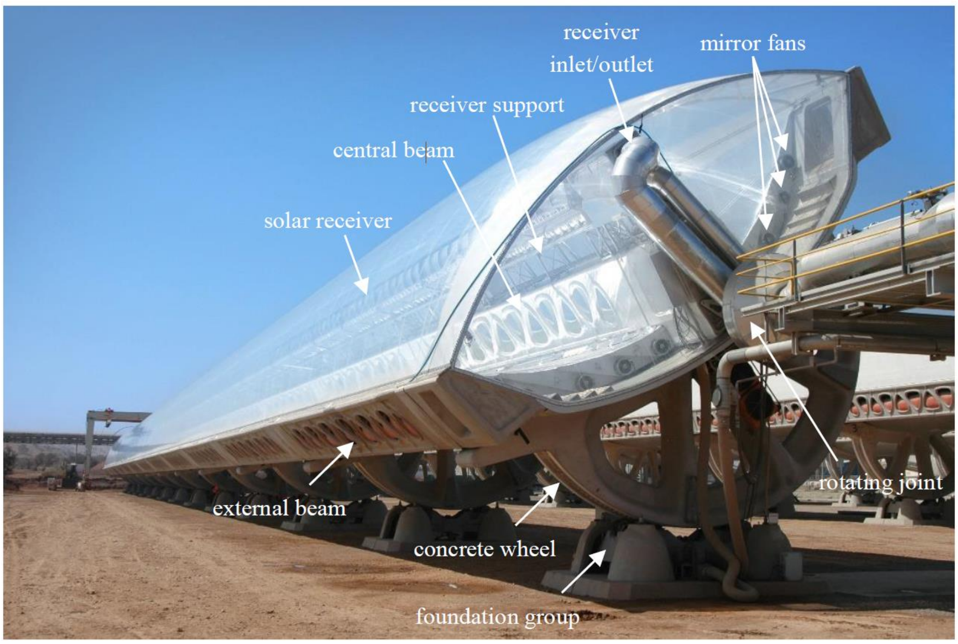

Figure 12 Pilot plant in Ait Baha, Morocco. Photograph of one solar collector unit in tracking mode.

A solar collector unit comprises 12 modules. Each module contains three 5.88 m-long sections. A photograph of an assembled solar receiver section is shown in Figure 13. The trumpet secondary concentrators are fabricated from 1.96 m-long extruded aluminum profiles featuring an internal channel for the cooling water flow. The feeding pipe is constructed from a steel grid that spans an airtight, temperature resistant tubular PTFE/glass fiber fabric. At the bottom, it features an axial, perforated steel plate with threads for the T-branches, denoted as T inlet plate. The knife gate valves are constructed by a second axial, perforated steel plate, referred to as knife blade, which is pushed onto the T inlet plate by springs while allowing for sliding. The position of the knife blade is controlled by a step motor for each receiver section. Thermal expansion of the feeding pipe is accounted for by expansion bellows placed between the receiver sections. The absorber tubes are fabricated from stainless steel (grade AISI 316L) and coated by black paint for enhanced solar absorptance. The collecting pipe is assembled from 2.94 m-long stainless steel (grade AISI 321) pipe segments, i.e., two segments per receiver section, each equipped with 13 expansion bellows. The thermal insulation layers on the feeding pipe, inner and outer surrounding groove walls, and on the collecting pipe are made of glass wool and Promaglaf HT. The radiation shield insulation is constructed from corrugated aluminum foils that are kept at the design distance by circumferential glass wool spacers placed in axial intervals of 0.5 m.

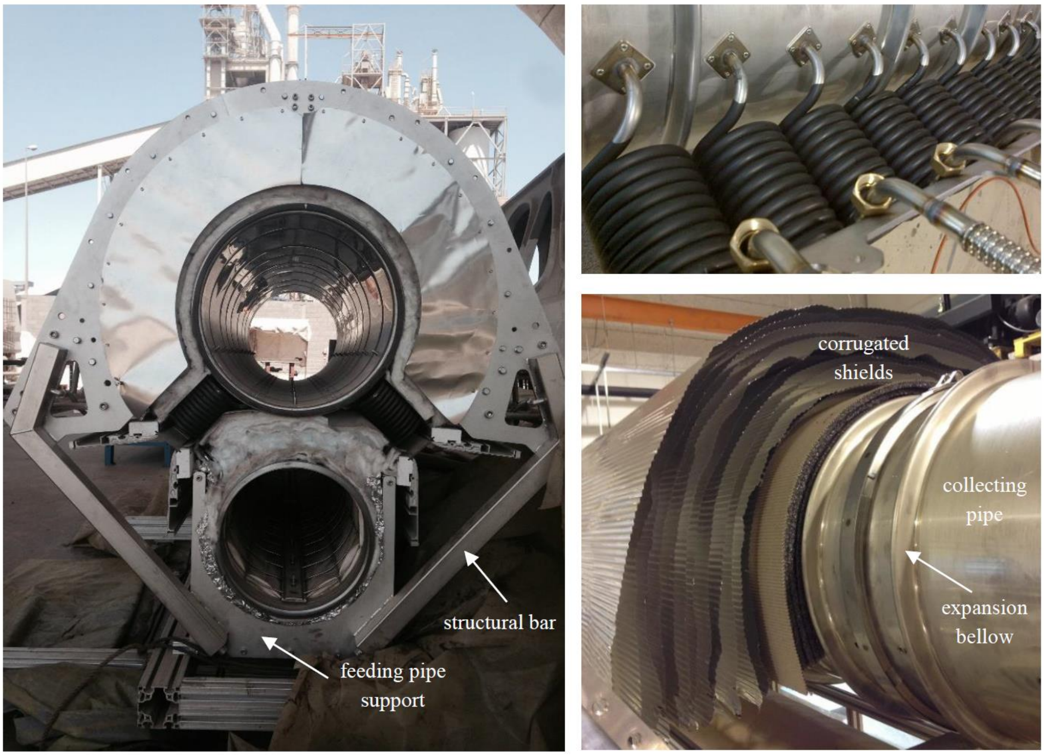

Figure 13: Photographs of a solar receiver section assembled on the ground (left), with an array of coiled absorber tubes (top right) and corrugated radiation shields (bottom right) attached to the collecting pipe.

A numerical optical and heat transfer analysis of the complete solar collector unit was formulated and experimentally validated by comparison to measured data collected during the commissioning phase of the first-of-its-kind solar pilot plant in Ait Baha, Morocco. The maximum and RMS percentage deviations between the measured and computed thermal power output of the solar concentrating system are 13% and 6%, respectively. For a yearly DNI of 2400 kWh/m^2, model simulations predict an annual thermal energy output at 500 °C of

926 kWh/m^2 of primary solar concentrator aperture. The validated optical and heat transfer models can be further applied for the design and optimization of the solar concentrating optics and solar receiver technology.

1.3.2. Arcspline solar concentrator

The pneumatic arcspline concentrator (ASC), identified as “primary concentrator” in Figure 10, has been designed for maximum intercept factor with the solar receiver’s secondary concentrator in a tilted focal plane. The theory of the film length regulation mechanism based on inflatable sleeves has been developed, including gravity effects. The weight of the film-sleeve-fixtures in the real system is found to distort the shape of the ASC significantly such that the optical design cannot be established in practice. In addition, concrete beam deflection, receiver displacement and temperature variations during solar tracking were found to decrease the concentrator’s performance. To overcome these challenges, a model-based control system is proposed that automatically adjusts the pressures.

1.3.3. Parametric study

The validated heat transfer model of the solar air receiver and solar concentrating optics, described in the first chapter of the BFE report of 2014, is applied to a parametric study of the new receiver design based on an array of coiled absorber tubes. From the geometric parameters that define the geometry of the helically coiled tubes, meaningful dimensionless numbers are defined. Numerical simulations are performed for various values of DNI and skew angle. The aim was to identify trends and peculiarities of the new solar trough receiver design and to find good parameters in terms of annual mean efficiency, material use and costs. Heat losses through the windowed aperture show a significant skew angle dependence due to the 3D nature of the coiled absorber tubes. This effect can be partially counteracted by tilting (skewing) the absorber tubes towards the skew rays of solar radiation. The robustness of the annual mean overall efficiency to the absorber tube geometry allows tuning for other design criteria such as material use and cost, e.g., by introducing gaps between the coils.

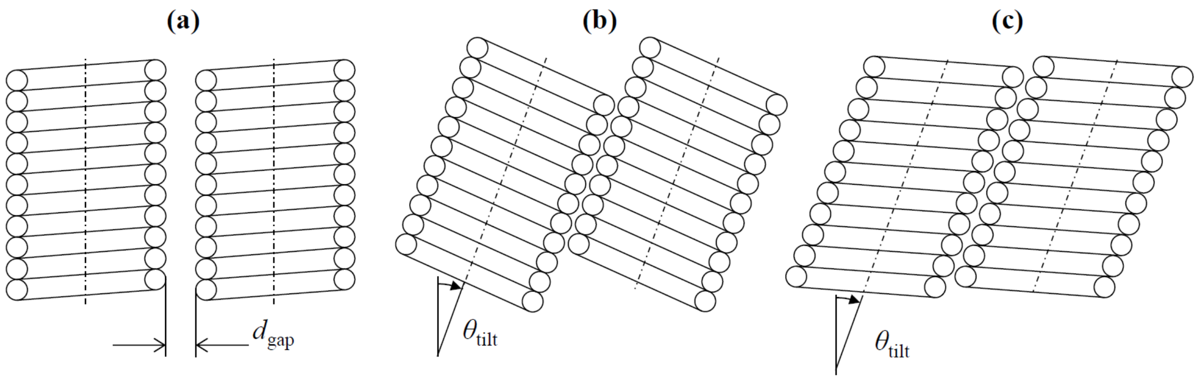

Figure 14: Schematic of the longitudinal section of array of absorber tubes selected for the analysis: (a) with gaps, (b) tilted absorber tubes, (c) and skewed absorber tubes.

1.3.4. Piping optimization

ModeFrontier software, developed by Esteco S.p.A., was exploited for the optimization of the peripheral portion of a CSP plant based on Airlight parabolic trough collectors, which were modelled in Simscape R2014b exploiting a custom domain for gases with temperature dependent properties. Two different approaches were followed: the first combined the original Simscape model and the MOGA algorithm, which was preferred for its robustness. Some interesting results were gathered introducing a synthetic objective function in which all the most meaningful outputs were combined and weighted in a cost function, to be minimized. This procedure led to a Pareto Front, a system of designs characterized by the same value of the objective function but in which with no further improvements were gatherable without a worsening of at least one of the other targets (i.e., heat losses and transient energy). A further step forward was made moving onto the second approach, introducing an annual simulation of the plant which included the solar power radiation variation and the thermal energy storage models. MOGA and MOPSO algorithms were employed to maximize the total revenues of the plant. The results from both the approaches have either some common features and, on the other hand, some remarkable differences:

- the diameter reduction from the TES towards the feeding line and the cold branches, and conversely its increase from hot branches back to TES, is a common feature in all the best designs in both the approaches;
- the solid insulation layer emerged only over the hotter sections of the piping lines;
- in the first optimum design the insulation of all the piping line is characterized by the lowest number of radiation shields combined with the largest air gaps. On the contrary, in the second approach the optimum insulating structure includes a higher number of shields, with air gaps large as in the previous solution. The cause can be found considering the transient behaviour assumption of the piping line, during which thermal losses warm up the structure. Heat losses and transient losses are coupled and are not minimized simultaneously, as in the first approach. Low heat losses determine higher transitory times; thus, the piping model is not able to reach its expected steady temperature during daily operations. This behaviour is caused by the heat fluxes values, assumed constant and equal to those at steady state condition. This simplification, implicitly adopted in the pseudo-transient approach, does not detect the early dynamics of the warming process, during which the high temperature gradients accelerate the establishment of a steady temperature profile within the insulating structure. In the first approach instead, heat losses and transient energy were accounted separately in the minimization function, assuming implicitly that the piping network reaches almost immediately its steady temperature profile.

The analysis was influenced by the assumptions on material costs, electrical prices and components efficiencies, which might be determinant in modification of the best piping configuration as much as the objective functions. Finally, technical constrains on the maximum weight and external diameters of the pipes would also limit the number of radiation shields. Since the present work highlights the relevance of heat losses and transient evolutions, some further investigations are required to define the best approach to weigh them into the annual simulation of the plant, and thus to confirm an optimum design of the piping network.

1.3.5. Thermal energy storage system

Experimental and CFD analysis of a combined sensible/latent heat TES

A 2D CFD model was developed with the aim of evaluating the performance of a combined sensible/latent heat TES (see Figure 4). Furthermore, a lab-scale combined TES prototype was exploited to assess the accuracy of the numerical model by comparing the CFD simulation results with experimental data.

The lab-scale combined TES prototype under investigation is depicted in Figure 15. A packed bed of gravel was exploited as sensible heat section of the TES. The average particles diameter and void-fraction were 32 mm and 0.4 respectively; the total packed bed mass was 245 kg. Concerning the latent heat section of the TES, $AlSi_{12}$ was selected as proper PCM material. The latter was encapsulated in AISI 316 steel tubes, 16 mm internal diameter and 1 mm thickness. The encapsulated PCM was positioned on top of the packed bed and distributed on four layers, constituted by 17 tubes each and oriented with an angle of 45°, forming a sort of tube bundle with an average void-fraction of 0.55. The total mass of the latent heat section of the TES was about 22.5 kg divided in 9.3 kg and 13.2 kg of PCM and encapsulation mass respectively. Pebbles and encapsulated PCM were located into a 1.68 m high cylindrical AISI 304 stainless steel tank, 0.4 m external diameter and 3 mm thickness, leading to a total height of 1.27 m and 0.09 m for the former and the latter respectively.

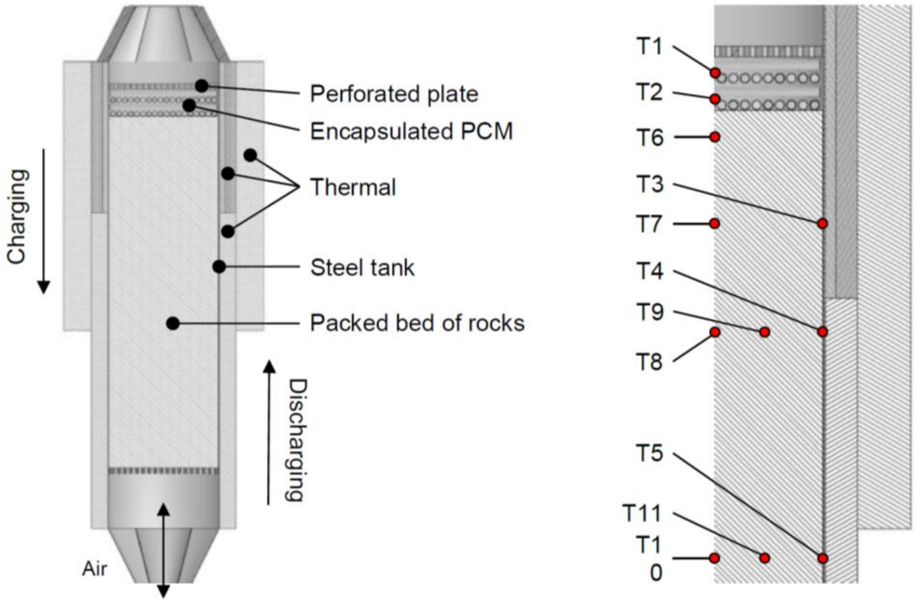

Figure 15: Schematic of the pilot-scale combined TES (l.h.s.) and TCS position (r.h.s.).

The purposely developed 2D CFD model of a lab-scale combined sensible/latent heat TES was satisfactorily validated with a reference set of experimental data gathered during one of the several experimental campaigns performed. The overall agreement between simulation results and experimental data is fairly good. However, further effort is still required to increase the accuracy of discharge phase results.

On the basis of the experimental data, the addition of a small amount of PCM on top of the packed bed seems to be a promising solution for stabilizing the HTF outflow temperature during discharging. Furthermore, due to the small tank-to-particle diameter ratio, the thermo-fluid dynamics behavior of the combined TES prototype was significantly affected by the radial variation of the void-fraction.

Performance evaluation of the Ait-Baha pilot plant TES system

The TES unit of the Ait-Baha pilot plant was dimensioned to operate at temperatures up to 650°C leading hence to a system capacity of 100 MWh_{th}. Some pictures of the construction phase of the TES unit are reported in Figure 16.

Figure 16: Pictures of the TES unit during construction: top) first layer of rocks with thermocouples sustaining structure; middle) containing tank filled with rocks, bottom) TES system completed. (Courtesy of Airlight energy SA).

The thermo-fluid dynamics behaviour of the packed bed TES system, implemented in the Ait-Baha pilot plant, was evaluated exploiting a 2D CFD approach. The TES unit was analysed under 10 consecutive cycles constituted by 10 h of charging followed by up to 4.5 h discharging at most with higher HTF mass flow rate. The discharging duration was determined by the HTF outflow temperature which, for an efficient integration into the pilot plant, cannot be reduced by more than 35°C with respect to the nominal charging temperature of 570°C. A total of 30 h of pre-charging were assumed prior to the cyclic operation.

The CFD simulations results allowed to observe, during the first cycles, the presence of severe radial temperature gradients at the bottom of the packed bed which reduces as the consecutive cycles increases. The performance of the TES unit were evaluated on the basis of the first and the second law of thermodynamics; for both these figures of merit, a transient behaviour of the TES can be observed for all the cycles analysed achieving values larger than 75% after the 10th cycle.

Performance analysis of a packed bed TES system integrated in a compressed air energy storage plant

The feasibility of including a packed bed TES tank in a CAES plant to recover heat from the pressurized-air after the compression stage has been analysed in detail. In order to perform this analysis an innovative CFD model has been developed, which introduces all the governing heat transfer mechanisms that occur in packed bed TES systems (conductive, convective and radiative). Furthermore, all the implications derived from the TES operation under pressurized conditions are also accounted for.

Based upon the working condition of the Huntorf CAES plant, a packed bed TES system was proposed, dimensioned and evaluated from both the first and the second law of thermodynamics.

Due to the large amount of packing material required to store the given amount of energy, it was proposed to split the overall rocks volume into two tanks (first scenario) and four tanks (second scenario) in a parallel arrangement. By comparing the results obtained with those of the reference single-tank TES, it was possible to observe that the multiple-tank TES configuration has a minor influence on thermal stratification.

The TES system proposed, to evaluate the applicability in of the proposed TES system in a real CAES plant, a new CFD simulations was performed with the aim of studying the TES performance operating under realistic working conditions of partial charge and discharge phases based upon the availability/ requirement of electricity form the grid. Three partial charging (during period of low energy demand) and discharging (during peak period of energy demand) where considered for each day for a total of 31 days. According to the simulations results, after the first 6-7 days, a stable thermal stratification into the packed bed is obtained with the HTF outflow temperature during discharging always above the threshold value of 480 ºC. An unwanted increase of the HTF outflow temperature, up to 415°C, during the first charging was also observed due to the large TES pre-charging considered. Nevertheless, on average, the efficiency of the system resulted to be in the range of 96%.

1.4. Major achievements of the first year of the project (2017)

The aim of this paragraph is to provide an overview on the major results obtained during the third year of the project. The detailed description of the activities can be found in:

"SolAir-3: Innovative solar collectors for efficient and cost-effective solar thermal power generation – 3" (SI/500926-01), Annual report, December 2017.

1.4.1. Thermal energy storage system

Performance evaluation of the Ait-Baha pilot plant TES system

The TES system integrated in the Ait-Baha pilot plant was further studied exploiting the same 2D CFD-based approach previously developed. The TES unit was analysed under 60 consecutive cycles of 10 h charging followed by 4 h discharging, with higher HTF mass flow rate, and 10 h of idle. The real discharging duration of 4 h was determined by the HTF outflow temperature which, for an efficient integration into the pilot plant, cannot be reduced by more than 40-45°C with respect to the nominal charging temperature of 570°C. Since at the beginning of the simulation the TES unit was considered to be in thermal equilibrium with the environment, a total of 5 pre-charging cycles were assumed prior to the cyclic operation to reduce the initial transients. Furthermore, a parametric analysis was also performed with the aim of assessing the effect of parameters, such as (i) HTF discharging mass flow rate and (ii) particle size distribution into the packed bed, have on the overall TES cyclic performance.

An important result of the simulation is that a relatively weak thermal stratification into the packed bed characterizes the behaviour of the TES unit. In terms of HTF outflow temperature during discharging, a monotonic decrease was observed throughout the whole phase with a more pronounced reduction at the very beginning of the process indicating that the TES unit cannot provide a stable HTF outflow temperature. Conversely, an HTF outflow temperature increase during charging, up to 35°C at most above the nominal discharging temperature, was obtained; in this case also the thermocline is discharged from the beginning of the process.

The parametric analysis allowed to observe that HTF mass flow rate variation during discharging has a minor influence on the TES performance. Conversely, assuming a different particles size distribution into the packed bed allowed to obtain a slightly higher HTF discharging outflow temperature during the initial 10-15 cycles.

The performance of the TES unit was evaluated on the basis of the first- and the second-law of thermodynamics. The resulting transient performances of the TES unit showed a similar evolution increasing monotonically up to a stable value of about 90% and 88% for the energy and exergy efficiency respectively.

2. Publications

S.A. Zavattoni, G. Zanganeh, A. Pedretti, M.C. Barbato, “Numerical analysis of the packed bed TES system integrated into the first parabolic trough CSP pilot-plant using air as heat transfer fluid”, AIP Conference Proceedings 2033, 090027 (2018); doi: 10.1063/1.5067121

I. Ortega-Fernández, S.A. Zavattoni, J. Rodríguez-Aseguinolaza, B. D’Aguanno, M.C. Barbato, “Analysis of an integrated packed bed thermal energy storage system for heat recovery in compressed air energy storage technology”, Applied Energy 205 (2017), pp. 280–293; doi: http://dx.doi.org/10.1016/j.apenergy.2017.07.039

S.A. Zavattoni, L Geissbühler, M.C. Barbato, G. Zanganeh, A. Haselbacher, A. Steinfeld, “High-temperature thermocline TES combining sensible and latent heat - CFD modeling and experimental validation”, AIP Conference Proceedings 1850, 080028 (2017); doi: 10.1063/1.4984449

S.A. Zavattoni, M.C. Barbato, G. Zanganeh, A. Pedretti, “High temperature thermocline TES – effect of system pre-charging on thermal stratification”, AIP Conference Proceedings 1734, 050043 (2016); doi: 10.1063/1.4949141

P. Good, G. Ambrosetti, A. Pedretti, A. Steinfeld, "An array of coiled absorber tubes for solar trough concentrators operating with air at 600°C and above," Solar Energy Vol. 111, pp. 378-395, (2015).

S.A. Zavattoni, M.C. Barbato, A. Pedretti, G. Zanganeh, “Single-tank TES system – Transient evaluation of thermal stratification according to the second-law of thermodynamics”, Energy Procedia 69 (2015), pp. 1068 – 1077; doi: 10.1016/j.egypro.2015.03.213

S.A. Zavattoni, M.C. Barbato, A. Pedretti, G. Zanganeh, “Evaluation of thermal stratification of an air-based thermocline TES with low-cost filler material”, Energy Procedia 73 (2015), pp. 289 – 296; doi: 10.1016/j.egypro.2015.07.691

3. References

None

National cooperation

None

International cooperation

None